

## Supplementary information

# Speeding up Reconstruction of 3D Tomograms in Holographic Flow Cytometry via Deep Learning

Daniele Pirone,<sup>a,b</sup> Daniele Sirico,<sup>a</sup> Lisa Miccio,<sup>a</sup> Vittorio Bianco,<sup>a</sup> Martina Mugnano,<sup>a</sup> Pietro  
Ferraro<sup>‡,a</sup> and Pasquale Memmolo<sup>‡‡,a</sup>

<sup>a</sup> CNR-ISASI, Institute of Applied Sciences and Intelligent Systems "E. Caianiello", Via Campi Flegrei 34, 80078 Pozzuoli, Napoli, Italy.

<sup>b</sup> DIETI, Department of Electrical Engineering and Information Technologies, University of Naples "Federico II", via Claudio 21, 80125 Napoli, Italy.

‡ [pietro.ferraro@isasi.cnr.it](mailto:pietro.ferraro@isasi.cnr.it)

‡‡ [pasquale.memmolo@isasi.cnr.it](mailto:pasquale.memmolo@isasi.cnr.it)

## CAN performances at different widths

In Fig. S1 we assess the CAN performances at different widths  $w$ . In particular, we perform a mini-training of the  $w = 32$ ,  $w = 64$ , and  $w = 128$  architectures in order to compare their outputs. The central slice of the same cell shown in Fig. 5A is reported in Fig. S1A after reconstructing the tomogram by means of these three trained models. As also visible in the RI profiles displayed in Fig. S1B, the accuracy of the network in reconstructing the correct 3D RI tomogram increases with the width  $w$ , as expected. To quantify this property, we reconstruct again the 65 tomograms and for each of them we measure the average RI, the equivalent radius, the dry mass, and the standard deviation RI. The percentage errors between these features measured in the standard case and the same ones measured in the three CAN cases are reported in Fig. S1C, in which it can be noted the decreasing trend of the error as the width  $w$  increases. It is worth noting that, as the training dataset has been reduced by a quarter, the percentage errors reported in Fig. S1C regarding the  $w = 64$  architecture are bigger than the corresponding ones computed through the same architecture and reported in Figs. 5D-G. Nevertheless, the percentage errors of dry mass and standard deviation RI even reach a lower value in the case of the  $w = 128$  model trained with the reduced dataset with respect to the  $w = 64$  model trained with the entire dataset, i.e. 3.23% and 11.05%, respectively.

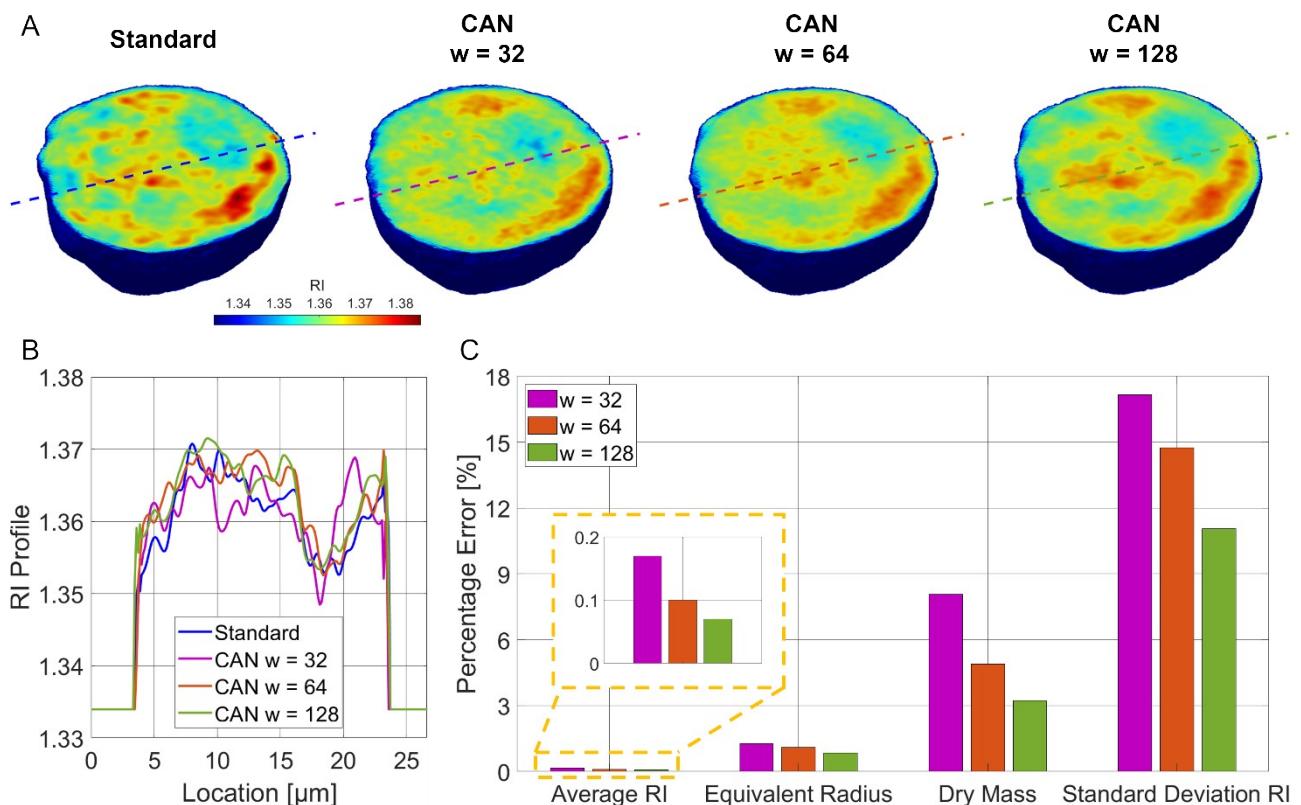


**Figure S1. Assessment of the CAN performances after a mini-training of the architecture at different widths  $w$ .** **A** Central slice of a 3D RI tomogram reconstructed by the standard method and the CAN method with  $w = 32$ ,  $w = 64$ , and  $w = 128$ . **B** RI profile corresponding to the lines highlighted in **A**. **C** Percentage errors between the average RI, the equivalent radius, the dry mass, and the standard deviation RI measured in 65 standard tomograms and the same features measured in the corresponding CAN tomograms obtained with  $w = 32$ ,  $w = 64$ , and  $w = 128$ . The percentage errors of the average RI are zoomed in the inset.

## Supplementary Video S1

Detection, raw tracking, and ROI selection of a flowing cell in the recorded DH sequence.